Mechanism of Human Aldehyde Reductase: Characterization of the Active Site Pocket†

Oleg A. Barski,‡ Kenneth H. Gabbay,‡,§ Charles E. Grimshaw,|| and Kurt M. Bohren*,‡

Molecular Diabetes & Metabolism Section, Departments of Pediatrics and Cell Biology, Baylor College of Medicine, Houston, Texas 77030, and the Whittier Diabetes Program, University of California at San Diego, La Jolla, California 92093-0983

Received April 28, 1995; Revised Manuscript Received June 26, 1995⊗

ABSTRACT: Human aldehyde reductase is a NADPH-dependent aldo−keto reductase that is closely related (65% identity) to aldose reductase, an enzyme involved in the pathogenesis of some diabetic and galactosemic complications. In aldose reductase, the active site residue Tyr48 is the proton donor in a hydrogen-bonding network involving residues Asp43/Lys77, while His110 directs the orientation of substrates in the active site pocket. Mutation of the homologous Tyr49 to phenylalanine or histidine (Y49F or Y49H) and of Lys79 to methionine (K79M) in aldehyde reductase yields inactive enzymes, indicating similar roles for these residues in the catalytic mechanism of aldehyde reductase. A H112Q mutant aldehyde reductase exhibited a substantial decrease in catalytic efficiency (k_{cat}/K_m) for hydrophilic (average 150-fold) and aromatic substrates (average 4200-fold) and 50-fold higher IC_{50} values for a variety of inhibitors than that of the wild-type enzyme. The data suggest that His112 plays a major role in determining the substrate specificity of aldehyde reductase, similar to that shown earlier for the homologous His110 in aldose reductase [Bohren, K. M., et. al. (1994) *Biochemistry 33*, 2021−2032]. Mutation of Ile298 or Val299 affected the kinetic parameters to a much lesser degree. Unlike native aldose reductase, which contains a thiol-sensitive Cys298, neither the I298C or V299C mutant exhibited any thiol sensitivity, suggesting a geometry of the active site pocket different from that in aldose reductase. Also different from aldose reductase, the detection of a significant primary deuterium isotope effect on k_{cat} (1.48 ± 0.02) shows that nucleotide exchange is only partially rate-limiting. Primary substrate and solvent deuterium isotope effects on the H112Q mutant suggest that hydride and proton transfers occur in two discrete steps with hydride transfer taking place first. Dissociation constants and spectroscopic and fluorimetric properties of nucleotide complexes with various mutants suggest that, in addition to Tyr49 and His112, Lys79 plays a hitherto unappreciated role in nucleotide binding. The mode of inhibition of aldehyde reductase by aldose reductase inhibitors (ARIs) is generally similar to that of aldose reductase and involves binding to the E:$NADP^+$ complex, as shown by kinetic and direct inhibitor-binding experiments. The order of ARI potency was AL1576 (K_i = 60 nM) > tolrestat > ponalrestat > sorbinil > FK366 > zopolrestat > alrestatin (K_i = 148 μM). Our data on aldehyde reductase suggest that the active site pocket significantly differs from that of aldose reductase, possibly due to the participation of the C-terminal loop in its formation.

Aldehyde reductase (EC 1.1.1.2) is one of several enzymes constituting the aldo−keto reductase superfamily that catalyzes the NADPH-dependent reduction of a wide variety of aldehydes (Bohren et al., 1989). A closely related member of this family, aldose reductase, is implicated in the pathogenesis of certain diabetic complications (Gabbay, 1973; Dvornik, 1987; Kador, 1988). The physiological role(s) of these and several other similar enzymes in this family has not yet been completely established, but they are thought to be involved in the detoxification and maintenance of specific control over the levels of reactive aldehydes (Bachur, 1976) and in osmoregulation within the renal tubular cells (Garcia-Perez & Burg, 1991) and many other cell types. Aldehyde and aldose reductase differ significantly in their substrate specificities and tissue distributions (Davidson et al., 1977; Wermuth, 1982), and despite similar kinetic mechanisms, there are nevertheless differences in the functions of the two enzymes that are not yet understood.

Aldose reductase was shown to follow a sequential ordered mechanism in which NADPH binds to the enzyme first and $NADP^+$ is released last after the alcohol product (Boghosian & McGuinness, 1981; Wermuth et al., 1982; Ryle & Tipton 1985; Tanimoto et al., 1986). The crystal structures of the nucleotide-free aldose reductase apoenzyme (Rondeau et al., 1992) and the holoenzyme (Wilson et al., 1992; Harrison et al., 1994) have been solved, and it is clear that the movement of a nucleotide-binding loop is necessary for cofactor binding and release. The enzyme conformational change(s) associated with the loop movement that precedes $NADP^+$ release is the rate-limiting step in the forward reaction (Grimshaw et al., 1989; Kubiseski et al., 1992). The reaction mechanism

† This work was supported by grants from the Juvenile Diabetes Foundation (O.A.B., K.H.G., and K.M.B.), the Charles E. Culpeper Foundation and the NIH (DK43595; C.E.G.), and the Harry B. and Aileen B. Gordon Foundation (K.H.G.).

* Address correspondence to this author at the Department of Pediatrics, Baylor College of Medicine, 1 Baylor Plaza, Houston, TX 77030; Telephone (713) 770-3759, FAX (713) 770-3766, e-mail kbohren@mbcr.bcm.tmc.edu.

‡ Department of Pediatrics, Baylor College of Medicine.

§ Department of Cell Biology, Baylor College of Medicine.

|| University of California at San Diego.

⊗ Abstract published in *Advance ACS Abstracts,* August 15, 1995.

0006-2960/95/0434-11264$09.00/0

involves a hydride transfer from NADPH to the carbonyl carbon of the substrate and a proton transfer from the Tyr48 residue at the bottom of the active site cavity, which serves as the general acid catalyst, to the forming alcohol group (Harrison et al., 1994; Bohren et al., 1994).

Close sequence similarity between aldose and aldehyde reductases suggests that aldehyde reductase may utilize mechanisms and form a tertiary structure similar to those of aldose reductase. Indeed, aldehyde reductase was also shown to follow a sequential ordered kinetic mechanism (Davidson & Flynn, 1979; De Jongh et al., 1987; Bhatnagar et al., 1988), and the 2.48 Å preliminary structure of the aldehyde reductase apoenzyme (El-Kabbani et al., 1994) showed it to have a β/α barrel motif similar to that shown earlier for the human aldose reductase apoenzyme and the intact aldose reductase/NADPH holoenzyme [Rondeau et al. (1992) and Wilson et al. (1992), respectively]. However, the structure of the active site pocket and its residues was not described and the coordinates were not made available for comparison with aldose reductase.[1] An earlier mutagenesis study in our laboratory showed that Lys262 is important for cofactor binding in both enzymes, but with slightly different effects (Bohren et al., 1991). These facts prompted us to carefully investigate recombinant human aldehyde reductase and its kinetic mechanism. In the present study we have identified the active site residues of aldehyde reductase and determined the binding of NADPH and $NADP^+$, as well as the inhibition by some classical aldose reductase inhibitors. The mutant enzymes Y49F, Y49H, K79M, H112Q, I298A, I298C, and V299C were overexpressed, purified, and characterized. The results are consistent with Tyr49 being the proton donor in the reduction reaction, while His112 and Ile298 are important for substrate interaction. We further show that nucleotide exchange is not as rate-limiting in aldehyde reductase as it is in aldose reductase and that hydride transfer is thus a more prominent rate-limiting step in the overall reaction. These differences appear to be related to the different functions of the nucleotide-holding loops in the two enzymes, a finding that may be of significance to the understanding and development of specific aldose and aldehyde reductase inhibitors.

MATERIALS AND METHODS

Expression and Purification of Wild-Type Aldehyde Reductase and Its Mutants. Construction of the wild-type human aldehyde reductase expression plasmid in the pET system was described previously (Bohren et al., 1991). Site-directed mutagenesis was performed with the Amersham mutagenesis kit in single-stranded M13, using oligomers with the required mismatches shown in Table 1. *Nco*I restriction sites were created on both ends of the mutant cDNA by polymerase chain reaction (PCR) in order to insert the amplified cDNA into the *Nco*I cloning site of the pET11d expression vector (Bohren et al., 1991). The recombinant plasmids were transformed into *Escherichia coli* strain BL21, and the enzyme proteins were overexpressed and purified as previously described (Bohren et al., 1991), with slight modifications, e.g., the concentration of the salt gradient during DEAE-Sephacel chromatography was increased to 0.12 M. For the purification of the I298C and V299C mutants, buffers containing 7 mM β-mercaptoethanol were used to protect against possible oxidation of the thiol groups.[2] Gel filtration on a P-10 column with ammonium sulfate was used to strip the cofactor from the purified protein as previously described (Ehrig et al., 1994). Alternatively, a pulse of 0.5 M NaCl was used instead of NADPH to elute coenzyme-free protein from the affinity column (Matrex Orange A, Amicon). During chromatography, enzymes were monitored by enzymatic assay or, in the case of the Y49F and K79M mutant proteins by SDS–polyacrylamide gel electrophoresis using the Phastsystem (Pharmacia) according to the manufacturer's instructions. SDS–polyacrylamide gel electrophoresis and Western blot analysis of all proteins were routinely performed after each purification as previously described (Bohren et al., 1991).

Table 1: Oligonucleotide Primers Used for Site-Directed Mutagenesis[a]

Y49F	5′	G	T	G	C	T	G	C	T	A	T	C	T	**T**	C	G	G	C	A	A	T	G	A	G	C	C	3′
Y49H	5′	G	T	G	C	T	G	C	T	A	T	C	**C**	A	C	G	G	C	A	A	T	G	A	G	C	C	3′
K79M	5′	G	T	G	A	C	A	T	C	C	A	**T**	G	C	T	G	T	G	G	A	A	C	A	C	C		3′
H112Q	5′	G	T	A	C	C	T	G	A	T	G	C	A	**G**	T	G	G	C	C	T	T	A	T	G	C	C	3′
I298A	5′	T	T	G	G	A	G	A	T	A	T	**G**	**C**	T	G	T	G	C	C	T	A	T	G	C	T		3′
I298C	5′	T	T	G	G	A	G	A	T	A	T	**T**	**G**	**C**	G	T	G	C	C	T	A	T	G	C	T		3′
V299C	5′	G	G	A	G	A	T	A	T	A	T	T	**T**	**G**	**T**	C	C	T	A	T	G	C	T	T	A		3′

[a] Underlined letters indicate base changes.

Enzyme Assays and Kinetic Analysis. Enzymatic activity was assayed during purification by measuring the rate of enzyme-dependent decrease in NADPH absorption at 340 nm in a Gilford Response spectrophotometer at 25 °C. The standard reaction mixture (1 mL volume) contained 0.2 mM NADPH, DL-glyceraldehyde, or D-glucuronate at various concentrations (depending on the mutant enzyme analyzed) in a 100 mM sodium phosphate buffer (pH 7.0). To measure the reverse reaction, 0.2 mM $NADP^+$ and varying concentrations of benzyl alcohol were used, and the increase in absorbance at 340 nm due to NADPH formation was followed. Each data point (initial velocity) was determined in duplicate over at least six different substrate concentrations. Control assays, lacking enzymes, were routinely included, and the rates, if any, were subtracted from the reaction rates. Kinetic constants were calculated by fitting the Michaelis–Menten function directly in the hyperbolic form to the data with an unweighted least-squares analysis using the Marquardt–Levenberg algorithm provided with Sigmaplot for Windows, version 1.02. Steady-state kinetics in the presence of inhibitors was analyzed by using

$$v_i = VA/[K_m(1 + I/K_{is}) + A(1 + I/K_{ii})] \quad (1)$$

where K_{is} is the slope (competitive) inhibition constant and K_{ii} is the intercept (uncompetitive) inhibition constant. The type of inhibition was determined according to the inhibition pattern and a relative difference between K_{is} and K_{ii}. If the difference was more than 10-fold, the term in eq 1 containing the higher constant value was set to 1, and the fit for either

[1] The atomic coordinates and structure factors of the human aldehyde reductase apoenzyme were embargoed by El-Kabbani et al. until November 1, 1995, and November 1, 1998, respectively.

[2] Site-directed mutagenesis was used to demonstrate that C298 is solely responsible for a reversible kinetic "thiol effect" in human aldose reductase. Some authors refer to this effect as "activated" and "unactivated" enzyme (Bohren & Gabbay, 1992).

K_{is} or K_{ii} improved significantly as judged from the standard errors and the sum of the residual least-squares values. If the difference between K_{is} and K_{ii} was less than 1.5-fold, the equation for noncompetitive inhibition was used ($K_i = K_{ii} = K_{is}$). The kinetic nomenclature used is that of Cleland (1963).

Determination of pH Profiles. pH profiles were determined over the range pH 5.5−10 using the following buffers: MES[3] (pH 5.5−6.5), MOPSO (pH 6.5−7.5), POPSO (pH 7.5−8.5), CHES (pH 8.5−9.5), and CAPSO (pH 9.5−10). Overlaps were used in all cases, and checks were made to ensure that none of the buffers were inhibitory and that at extreme pH's the enzyme was stable during the time needed for the measurements. The nucleotide concentration used was in all cases shown to be saturating (at least $20 \times K_m$). The pH profiles for k_{cat} and k_{cat}/K_m were fitted to eqs 2−4 (Cleland, 1977), which describe log Y vs pH curves that decrease above pK_2 (eq 2), decrease both below pK_1 and above pK_2 (eq 3), and level off at both low and high pH (eq 4). In eqs 2−4, Y is k_{cat} or k_{cat}/K_m, H is [H$^+$], and Y_{max} or Y_{min} is the maximal or minimal value of Y, respectively. The points in the figures (Figure 2) are the experimentally determined values, while the curves are calculated from fits of these data to the appropriate equations.

$$\log Y = \log[Y_{max}/(1 + K_2/H)] \quad (2)$$

$$\log Y = \log[Y_{max}/(1 + H/K_1 + K_2/H)] \quad (3)$$

$$\log Y = \log [(Y_{max} + Y_{min}K_2/H)/(1 + K_2/H)] \quad (4)$$

Studies of Substrate and Solvent Isotope Effects. NADPH and NADPD labeled with deuterium in the *pro-R* position were synthesized from unlabeled and 2-deuterio-L-malate using malic enzyme by the method of Viola et al. (1979) and purified by FPLC on a Mono-Q column using the procedure of Orr and Blanchard (1984). Primary deuterium isotope effects[4] on k_{cat} and k_{cat}/K_m for DL-glyceraldehyde were measured by direct comparison at saturating NADPH/D concentrations in 50 mM MOPSO (pH 7.0) buffer at 25 °C. Initial velocities, corrected for background, were fitted to

$$v_i = VA/[K_m(1 + F_iE_{k_{cat}}/K_m) + A(1 + F_iE_{k_{cat}})] \quad (5)$$

where F_i is the fraction of deuterium in the NADPH/D cofactor, $E_{k_{cat}}/K_m$ and $E_{k_{cat}}$ are the isotope effects minus 1 on k_{cat}/K_m and k_{cat}, respectively, and the other kinetic parameters are as described earlier by the nonlinear least-squares method and using the Fortran programs of Cleland (1979).

Solvent isotope effects on k_{cat} and k_{cat}/K_m for DL-glyceraldehyde were measured in a similar manner by direct comparison of initial velocities determined at a saturating NADPH concentration. Buffers made in D_2O were adjusted with NaOD to the desired "pH" by using a formula (pD = meter reading + 0.4) that corrects for the isotope effect on the response of the glass electrode (Salomaa et al., 1964). Initial velocity data were similarly fitted to eq 5. For the H112Q mutant, the $E_{k_{cat}}/K_m$ value appeared to be 0 (i.e., no solvent isotope effect on k_{cat}/K_m), so the data were fitted to the equation not containing this term.

Determination of Coenzyme Binding. To determine coenzyme binding constants of the wild-type and mutant aldehyde reductase enzymes, quenching of protein fluorescence upon titration by coenzyme was followed by using an Aminco Bowman Series 2 luminescence spectrophotometer with a thermostated cell compartment. Titrations were done at a protein concentration of approximately 0.1 mg/mL in 5 mM sodium phosphate buffer (pH 7.5) at 20 °C. Fluorescence spectra were taken after each addition of coenzyme using an excitation wavelength of 290 nm (2 nm bandwidth) and emission wavelengths of 315−400 nm (4 nm bandwidth). Fluorescence data at the emission wavelength of 373 nm were used for calculations to minimize inner filter effects. Due to the necessity to use high concentrations of NADPH to reach saturation in the case of the K79M mutant enzyme, corrections for inner filter effect were made using tryptophan titration (Birdsall et al., 1983). A tryptophan solution giving approximately the same fluorescence as the enzyme solution was titrated with NADPH under exactly the same conditions. Correction factors were determined by the division of initial tryptophan fluorescence intensity by fluorescence intensity at a specific NADPH concentration. Data from the enzyme titration were then multiplied by the corresponding correction factors to give the corrected fluorescence.

The fractional saturation, R, by coenzyme of the total coenzyme-binding sites was equated to the ratio $\Delta F/\Delta F_{max}$, where ΔF is the amount of fluorescence reduction at the specified coenzyme concentration and ΔF_{max} is the maximal amount of fluorescence reduction at fully saturating coenzyme concentrations. Although saturation was reached in all cases, ΔF_{max} was estimated by fitting the ΔF vs coenzyme concentration data to

$$\Delta F = \Delta F_{max}L/(K + L) \quad (6)$$

where L is the total coenzyme concentration and K is the half-saturation constant. The dissociation constant was evaluated by a variation of the Scatchard plot fitting the data to

$$1/(1 - R) = L/RK_d - E/K_d \quad (7)$$

where K_d is the dissociation constant and E is the total active site concentration (Stinson & Holbrook, 1973). Ideally, a plot of $1/(1 - R)$ vs L/R yields a straight line for a homogeneous receptor, with the slope equal to the reciprocal dissociation constant ($1/K_d$) and the abscissa intercept equal to the concentration of binding sites. Sigmaplot (version 1.02) for Windows was used for all calculations.

Determination of AL1576 Binding by Ultrafiltration Assay. The binding of AL1576 to aldehyde reductase was directly assessed by determining the unbound fraction of the inhibitor in an ultrafiltration assay (Ehrig et al., 1994). A spun microconcentrator with a molecular mass cutoff of 10 kDa (Centricon 10, Amicon) was used to separate free from

[3] Abbreviations: MES, 2-(*N*-morpholino)ethanesulfonic acid; MOPSO, 3-(*N*-morpholino)-2-hydroxypropanesulfonic acid; POPSO, piperazine-*N*,*N*′-bis(2-hydroxypropanesulfonic acid); CHES, 2-(*N*-cyclohexylamino)ethanesulfonic acid; CAPSO, 3-(cyclohexylamino)-2-hydroxy-1-propanesulfonic acid.

[4] Nomenclature: The isotope effect nomenclature is that of Northrop (1977), in which a leading superscript indicates the isotope effect being studied. Thus, $^{D}k_{cat}$ and $^{D}k_{cat}/K_m$ are primary deuterium isotope effects (that is, the value for the hydrogen-containing molecule divided by the value for the deuterated molecule) on the respective parameters. Similarly, $^{D_2O}k_{cat}$ and $^{D_2O}k_{cat}/K_m$ are the solvent isotope effects on the same parameters.

enzyme-bound ligands. The Centricon membrane was preadsorbed with the ligand by filtering 0.5 mL of 5 μM AL1576 solution to exclude AL1576 adsorption by the membrane during the assay. A volume of 1 mL of binding assay mixture was then added to the upper chamber of the concentrator, and approximately 250 μL was filtered through the membrane. The assay mixture contained 5 μM AL1576, aldehyde reductase, and either no coenzyme or 20 μM NADPH or $NADP^+$ in 5 mM sodium phosphate buffer (pH 7.5). The aldehyde reductase active site concentrations used were 10 μM for the wild type and the H112Q mutant and 7 μM for the Y49H mutant. Control assays containing only buffer or AL1576 were also done. The filtrate (250 μL) was diluted to 2 mL, and the concentration of AL1576 was determined fluorimetrically with excitation and emission wavelengths of 280 and 333 nm, respectively, using a calibration curve. Due to preadsorption with AL1576, a small amount bled from the membrane in control assays where only buffer was used in the upper chamber, and the fraction of unbound inhibitor was corrected accordingly for this bleeding.

Estimation of Cofactor Binding to Y49F Mutant Enzyme by Ultrafiltration Assay. Since the protein fluorescence of the Y49F mutant enzyme was minimally quenched by nucleotides, estimation of cofactor binding in this mutant was assayed directly by the same ultrafiltration principle that was used to assay the binding of AL1576. Centricons were preadsorbed with 5 μM NADPH or $NADP^+$. The Y49F enzyme (13 μM) and 8 μM nucleotide in 5 mM phosphate buffer were used in the ultrafiltration experiment. Control experiments with only buffer or only nucleotide were also included. The concentrations of nucleotides in the filtrates were determined spectroscopically at 260 and 340 nm.

Spectroscopic Measurements. Absorbance spectra were measured on a Gilford Response spectrophotometer at 25 °C. For measurement of the enzyme:$NADP^+$ complex, the cofactor concentration was 50 μM, and the protein concentrations of the wild type and the H112Q and K79M mutants were 37, 19, and 16 μM, respectively. To obtain difference spectra, the mixture of enzyme and $NADP^+$ was placed in the sample cuvette and the apoenzyme of the same concentration was placed in the reference cuvette (for the wild-type enzyme), or alternatively the absorbance of the apoenzyme was subtracted mathematically from the spectrum of the enzyme:$NADP^+$ complex (for H112Q and K79M mutants).

Protein Concentration. The purified enzyme protein concentration was determined from the absorbance at 280 nm and by using the method of Bradford (BioRad protein determination kit) with bovine γ-globulin as standard. The extinction coefficient of each nucleotide-free protein was calculated according to Gill and von Hippel (1989). The spectroscopic method yielded less protein than the Bradford method by a factor of 2.4 ± 0.3, but agreed well with the active site titrations. The calculated kinetic parameters are nevertheless based on the Bradford method in order to be consistent with our earlier publications.

RESULTS

Expression and Purification of Enzyme Proteins. The wild-type enzyme was readily expressed at high yields of ~40 mg/3 L preparation. Expression of the Y49F mutant gave low yields (3−5 mg/3 L preparation), as did the K79M mutant enzyme (3−6 mg/3 L preparation). The K79M mutant protein bound poorly to the affinity column, but was sufficiently retarded on the column to provide an apparently homogeneous protein, as judged by SDS−PAGE. For the purification of I298C and V299C mutants, buffers containing 7 mM β-mercaptoethanol were used to prevent the possible oxidation of these putative active site thiol groups whose oxidation states affect the kinetic characteristics in the homologous aldose reductase.[2] The H112Q, Y49H, I298A, I298C, and V299C mutants gave better yields of 25−50 mg/3 L preparation. These proteins were purified to homogeneity as determined by SDS−PAGE (Figure 1A) and reacted identically with antibodies against aldehyde reductase on Western blots (Figure 1B).

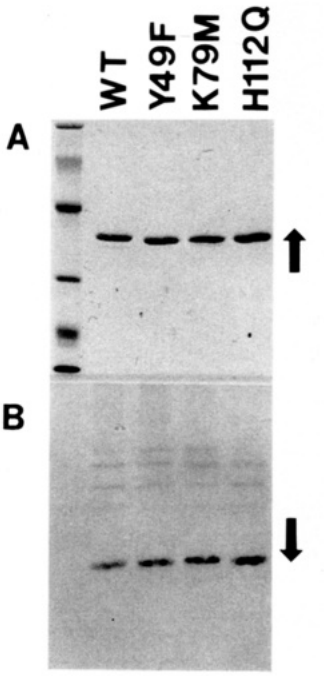

FIGURE 1: SDS−polyacrylamide gel electrophoresis (A) and Western blot analysis (B) of the purified wild-type aldehyde reductase and its mutants. (A) 1.5 μg of denatured protein was applied to a 12.5% homogeneous SDS PhastGel and stained with Coomassie Brilliant Blue R. Left lane, molecular mass standards: lysozyme (14.4 kDa), soybean trypsin inhibitor (21.5 kDa), carbonic anhydrase (31 kDa), ovalbumin (45 kDa), bovine serum albumin (66.2 kDa), and phosphorylase *b* (92.5 kDa). (B) Western blot analysis of gel identical to (A) probed with an antibody to human recombinant aldehyde reductase. The weak extra bands appearing on the Western blots are most probably due to mild bacterial protein contamination reacting strongly with our polyclonal antibody raised in rabbits using complete Freund's adjuvant. Arrows on the right indicate the direction of electrophoresis.

Kinetic Characterization of Tyr49 and Lys79 Mutant Enzymes. The Y49F and Y49H mutants exhibited no activity with any of the following substrates, DL-glyceraldehyde (up to 100 mM), D-glucuronate (up to 100 mM), *p*-nitrobenzaldehyde (up to 0.9 mM), or *p*-carboxybenzaldehyde (up to 0.9 mM), using a protein concentration of 0.2 mg/mL. The K79M mutant was also completely inactive with these substrates. The lowest detectable activity under our experimental conditions corresponds to 2.5×10^{-3} s^{-1}, which would be an upper limit for k_{cat} for these mutants.

Kinetic Characterization of the I298A, I298C, V299C, and H112Q Mutant Enzymes. Steady-state kinetic parameters of the wild-type aldehyde reductase and H112Q, I298A,

Table 2: Kinetic Constants of Wild-Type and Mutant Aldehyde Reductases[a]

	wild-type	I298A	ratio WT/I298A	I298C	ratio WT/I298C	V299C	ratio WT/V299C	H112Q	ratio WT/H112Q
DL-glyceraldehyde									
k_{cat}	1.3	2.1	0.641	3.4	0.38	1.2	1.07	0.21	6.1
K_m	1.7	33	0.05	11.5	0.15	1.8	0.89	76	0.02
k_{cat}/K_m	786	61	13	294	2.7	654	1.2	2.8	277
D-glucuronate									
k_{cat}	2.7	3.8	0.69	6.2	0.44	3.4	0.79	0.97	2.7
K_m	4.2	26.3	0.16	19.5	0.21	4.2	1	48	0.09
k_{cat}/K_m	637	146	4.3	320	2	809	0.79	20	32
succinic semialdehyde									
k_{cat}	3.7	3.72	1.0	6.2	0.6	2.9	1.27	0.28	13
K_m	0.17	2.8	0.06	1.5	0.1	0.41	0.42	18	0.01
k_{cat}/K_m	22186	1320	17	4185	5.3	7241	3.06	16	1403
p-nitrobenzaldehyde									
k_{cat}	5.1	3.0	1.74	4.4	1.16	4.7	1.09	0.056[b]	93
K_m	0.16	2.8	0.06	1.2	0.13	0.38	0.89	5.9[b]	0.03
k_{cat}/K_m	32025	1076	30	3717	8.6	12443	1.2	9.5	3377
p-carboxybenzaldehyde									
k_{cat}	3.7	5.8	0.64	5.9	0.63	3.7	0.99	0.054	69
K_m	0.038	0.38	0.1	0.43	0.09	0.1	0.39	2.8	0.01
k_{cat}/K_m	97534	15256	6.4	13575	7.2	38049	2.56	19	5129

[a] k_{cat} is expressed in s^{-1}, K_m is in mM, and k_{cat}/K_m is in s^{-1} M^{-1}. Standard errors for k_{cat} and k_{cat}/K_m did not exceed 10% and for K_m 20%, except where indicated. [b] Standard error is 36%.

and I298C mutants are summarized in Table 2. The wild-type enzyme has higher catalytic efficiency (k_{cat}/K_m) for hydrophobic substrates, such as *p*-nitrobenzaldehyde and *p*-carboxybenzaldehyde, than for polar substrates, such as DL-glyceraldehyde and D-glucuronate. The catalytic efficiency for succinic semialdehyde is intermediate between those of aromatic and hydrophilic substrates, which is consistent with its structure. The I298A mutant has k_{cat} values for all substrates that are comparable to those of the wild-type enzyme, while the K_m values are increased 6−20-fold and the catalytic efficiencies are decreased accordingly. Similarly, the I298C mutant has 2−5-fold higher catalytic efficiency than the I298A mutant for all substrates except *p*-carboxybenzaldehyde, which is identical for the two mutants. Unlike the Cys298 residue in aldose reductase, mutation of the corresponding aldehyde reductase residue, Ile298, to alanine or cysteine has an insignificant effect on the overall enzymatic activity, with the reduction of D-glucuronate and *p*-carboxybenzaldehyde affected least. The V299C mutant has kinetic parameters very similar to those of the wild-type enzyme. Since the Cys298 residue is responsible for the thiol sensitivity of aldose reductase, we tested whether the introduced thiol groups in the I298C and V299C mutants made these enzymes thiol-sensitive (Bohren & Gabbay, 1993). The mutant enzymes were dialyzed extensively (48 h) against buffer with or without 10 mM β-mercaptoethanol, and K_m and k_{cat} were measured using DL-glyceraldehyde as a substrate. As for wild-type aldehyde reductase, the mutant enzymes did not display any thiol sensitivity.

The mutation of His112 to glutamine has a drastic effect on enzymatic activity, with the catalytic constant, k_{cat}, decreasing by 6−100-fold while the K_m increases by 10−100-fold, depending on the substrate. These changes are reflected in severe decreases in catalytic efficiency (k_{cat}/K_m) of 30−5000-fold, with aromatic substrates like *p*-nitrobenzaldehyde and *p*-carboxybenzaldehyde most drastically affected (3400- and 5100-fold, respectively), while polar substrates such as DL-glyceraldehyde and D-glucuronate are much less affected (277- and 32-fold, respectively). The catalytic efficiency ratio for *p*-carboxybenzaldehyde/DL-glyceraldehyde is ~125 for wild-type enzyme, while the same ratio for the H112Q mutant decreases to 7. These findings suggest that His112 influences the accommodation and chemistry of interaction with aromatic and polar substrates in the active site pocket.

pH Profiles of Wild-Type and H112Q Mutant Enzymes. To further examine these interactions, we determined the pH profiles of the wild-type and H112Q mutant aldehyde reductases, using *p*-carboxybenzaldehyde and DL-glyceraldehyde as substrates (Figure 2). The k_{cat}/K_m profiles for the reduction of both substrates by the wild-type aldehyde reductase exhibit a break point in the basic region with pK = 9.4−9.6. The acidic region of the curve, with DL-glyceraldehyde as a substrate, has a break point with a pK = 6.3, whereas the curve with *p*-carboxybenzaldehyde is flat. This downward break of 1.5 log units with DL-glyceraldehyde, although defined by a single experimental point, cannot be attributed to enzyme inactivation at low pH, since a similar curve with *p*-carboxybenzaldehyde serves as a control and does not exhibit any drop at pH 5.5. These findings are consistent with the protonation of His112 at acidic pH, which weakens the DL-glyceraldehyde interaction with the enzyme active site, while the binding of *p*-carboxybenzaldehyde is not affected as it does not have a hydroxyl group at the C2 position to interact with His112 (see Discussion). The k_{cat}/K_m profile for the H112Q mutant with DL-glyceraldehyde shows only a single break point at pK = 9.5. In the acidic region the profile exhibits a slight (0.6 log unit maximum) negative deviation, which occurs gradually starting at neutral pH and therefore may be caused by low pH sensitivity of the H112Q mutant enzyme. This deviation thus does not constitute a break point and cannot be attributed to the ionization of any single group. Thus, the absence of an ionizable group at residue 112 eliminates the acidic break point, which is consistent with His112 interacting with the C2-hydroxyl of DL-glyceraldehyde. The pH dependency of k_{cat} for the wild-type enzyme, using both substrates, shows a wave-shaped profile that levels off at both high and low pH. It was not possible to measure k_{cat} using DL-glyceral-

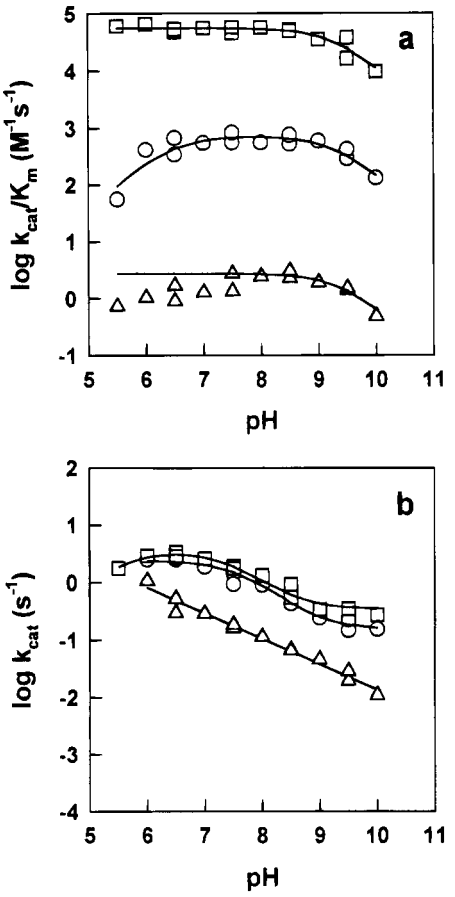

FIGURE 2: Effect of pH on log k_{cat}/K_m (a) and log k_{cat} (b) for the reduction reaction catalyzed by aldehyde reductase: ○, wild-type enzyme with DL-glyceraldehyde as substrate; □, wild-type enzyme with *p*-carboxybenzaldehyde as substrate; △, H112Q with DL-glyceraldehyde as substrate.

Table 3: Primary Deuterium and Solvent Isotope Effects for DL-Glyceraldehyde Reduction

	wild-type	H112Q
$^{D}(k_{cat})$	1.48 ± 0.02	1.79 ± 0.21
$^{D}(k_{cat}/K_m)$	2.28 ± 0.05	2.30 ± 0.15
$^{D_2O}(k_{cat})$	1.06 ± 0.03	2.06 ± 0.09
$^{D_2O}(k_{cat}/K_m)$	2.02 ± 0.06	0.96 ± 0.11

dehyde as a substrate at pH's below 6 due to a very high K_m (K_m > 50 mM). The k_{cat} profile of the H112Q mutant enzyme shows a straight line decreasing with increasing pH. The common characteristic of the k_{cat} profiles is a slope of 0.5 instead of the expected 1, indicating that complex kinetics and possible isomerization determine this catalytic constant.

Isotope Effects. The wild-type aldehyde reductase shows significant primary deuterium isotope effects on both k_{cat} and k_{cat}/K_m, determined by using NADPH and NADPD with DL-glyceraldehyde as a substrate (Table 3). There is a significant primary isotope effect on k_{cat} (1.48 ± 0.02) at pH 7.0, suggesting that the hydride transfer step is partially rate-limiting for the overall reaction. The proton transfer step, on the other hand, is less rate-limiting than hydride transfer, as demonstrated by the smaller solvent isotope effect on k_{cat} ($^{D_2O}k_{cat}$ = 1.06 ± 0.03). The solvent isotope effect on k_{cat}/K_m ($^{D_2O}k_{cat}/K_m$ = 2.02 ± 0.06) is similar to the substrate isotope effect ($^{D}k_{cat}/K_m$ = 2.28 ± 0.05), indicating that proton transfer is also a significant rate-limiting step for the overall reaction. The smaller magnitudes of the isotope effects on k_{cat} than on k_{cat}/K_m reflect the partial rate limitation of the overall reaction by cofactor exchange.

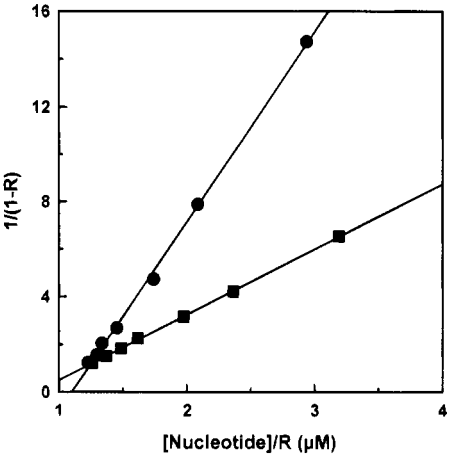

FIGURE 3: Linear transformation of the data on NADPH (●) or $NADP^+$ (■) binding to the wild-type aldehyde reductase. Initial data were obtained by measuring the quenching of enzyme fluorescence by the nucleotide as described in the Materials and Methods section. *R* stands for the degree of fluorescence quenching $\Delta F/\Delta F_{max}$.

Table 4: Coenzyme Binding to Aldehyde Reductase[a]

enzyme	K_{dNADPH} (μM)	NADPH quenching (%)	K_{dNADP^+} (μM)	$NADP^+$ quenching (%)	ϵ_{300}[b] (M^{-1} cm^{-1})
wild-type	0.13	87	0.36	76	562
Y49F	0.15	68	3.2	42	n/d[c]
Y49H	0.005	89	1.32	64	430
K79M	1.26	33	0.16	20	0
H112Q	0.011	85	1.78	65	465
I298A	0.19	85	0.60	51	n/d
I298C	0.42	90	1.32	62	470
V299C	0.10	88	0.72	76	n/d

[a] Standard errors for K_d and quenching were less than 10%. [b] ϵ_{300}: extinction coefficient of the $NADP^+$ perturbation band of the E:$NADP^+$ complex at 300 nm. [c] n/d, not determined.

The H112Q mutant also exhibits primary deuterium isotope effects on both k_{cat} and k_{cat}/K_m of the same extent as that of the wild-type enzyme (Table 3). Solvent isotope measurements using D_2O have a very significant effect (>2) on k_{cat} ($^{D_2O}k_{cat}$ = 2.06 ± 0.09), suggesting that the proton transfer step is rate-limiting for the overall reaction. However, the absence of a solvent isotope effect on k_{cat}/K_m ($^{D_2O}k_{cat}/K_m$ = 0.96 ± 0.11) implies that the mechanism of the H112Q mutant is changed and differs from that of the wild-type enzyme.

Nucleotide Binding. Binding constants were determined by fluorescence titration of the enzyme proteins with NADPH or $NADP^+$ (Figure 3). Maximal quenching of enzyme fluorescence by NADPH was generally greater than that by $NADP^+$. The nucleotide binding constants of the various mutants are presented in Table 4. Dissociation constants of NADPH or $NADP^+$ for the wild-type aldehyde reductase are in the submicromolar range and are virtually unchanged in the I298A and V299C mutant enzymes, but slightly elevated in the I298C mutant.

The dissociation constant for NADPH (K_{dNADPH}) of the Y49F mutant is virtually identical to that of the wild-type enzyme, although K_{dNADP^+} is increased to 3.2 μM, which is 10 times higher than the value of the wild-type protein. The

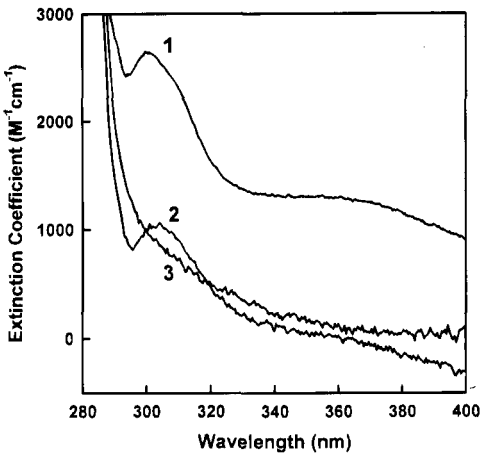

FIGURE 4: Difference absorbance spectra of the enzyme:$NADP^+$ complex vs apoenzyme: 1, wild-type aldehyde reductase; 2, H112Q mutant; 3, K79M mutant.

Y49H mutant, on the other hand, has a much tighter binding of NADPH with a K_d of 5 nM, while the K_{dNADP^+} is increased to 1.32 μM. Similarly, substitution of His112 by glutamine caused tighter binding of NADPH with a concomitant loosening of $NADP^+$ binding, as reflected by their respective K_d's (Table 4). In contrast, K_{dNADPH} for the K79M mutant was 10 times higher than that for the wild-type enzyme, while K_{dNADP^+} was 2 times lower (1.26 and 0.16 μM, respectively). As a result, the K79M mutant prefers $NADP^+$ over NADPH, a situation opposite that observed with the wild-type or any of the other mutant enzymes. Repulsion between the positive charges of Lys79 and the nicotinamide ring may be responsible for this change in preference.

The binding of nucleotides to Y49F was confirmed by an ultrafiltration assay. The assay (Ehrig et al., 1994) measures the free nucleotide in the ultrafiltrate of a mixture containing known amounts of nucleotide-free enzyme protein and nucleotide (see Materials and Methods). Binding of NADPH by the Y49F apoenzyme was complete, whereas a large proportion of the $NADP^+$ remained unbound and was found in the ultrafiltrate. The K_{dNADP^+} determined by this assay was estimated to be 6.9 μM, which is in good agreement with the value obtained by the fluorescence technique (3.2 μM). The ultrafiltration technique can only give estimates for the value of K_d due to errors associated with the preequilibration of the membrane and subsequent leaching of nucleotide.

The degree of quenching of protein fluorescence by both oxidized and reduced nucleotides is drastically reduced in the K79M mutant protein (Table 4), suggesting the importance of Lys79 in the mode of nucleotide binding. This conclusion is supported by the absence of a 300 nm band from the difference absorption spectrum of the K79M:nucleotide complex (Table 4). Figure 4 shows the difference spectrum of the aldehyde reductase:nucleotide complex, with a narrow band at 300 nm that is absent from the individual spectra of either enzyme or nucleotide alone. The band is similar to that observed in glutamate dehydrogenase complexed with NADPH (Pantaloni & Dessen, 1969) and apparently arises from the perturbation of cofactor or enzyme chromophores due to the E:NADPH interaction (Rizzo et al., 1987). This 300 nm band is therefore characteristic for the mode of cofactor binding, and its extinction coefficients for some of the mutant aldehyde reductases are given in Table 4. The absence of this band from the K79M mutant and the low degree of fluorescence quenching suggest an altered interaction of $NADP^+$ with the energy-transferring groups of this mutant. These changes in the mode of binding are not necessarily reflected in the binding affinity of nucleotides.

Table 5: Binding of AL1576 to Aldehyde Reductase Determined by Ultrafiltration Assay[a]

coenzyme	fraction of free AL1576 (%)	
	wild-type	Y49H
no coenzyme	95	120
20 μM NADPH	27	120
20 μM $NADP^+$	0.3	21

[a] One milliliter assays were analyzed for free AL1576 by filtering 250 μL through a Centricon 10 ultrafiltration membrane. The concentration of AL1576 in the filtrate was determined from its fluorescence at excitation and emission wavelengths of 280 and 333 nm, respectively. The assays contained 10 and 7 μM wild-type and mutant enzymes, respectively, 5 μM AL1576, and coenzyme.

Table 6: Inhibition of Aldehyde Reducatse, Its H112Q Mutant, and Aldose Reductase by ARIs[a]

inhibitor	IC_{50} (μM)			
	aldehyde reductase	H112Q mutant	aldose reductase[b]	ratio aldehyde/aldose
AL1576	0.06	3.0	0.8	0.075
tolrestat	0.72	63	0.01	72
ponalrestat	4.6	268	1.2	3.8
sorbinil	5.4	250	2	2.7
FK366	14.5	318	0.4	36
zopolrestat	27.0	185	0.06	450
alrestatin	148		1	148

[a] IC_{50}s for wild-type aldehyde reductase were measured with 3 mM DL-glyceraldehyde and 0.2 mM NADPH. For the H112Q mutant, the DL-glyceraldehyde concentration was 75 mM. [b] Data from Ehrig et al. (1994).

Inhibition of Aldehyde Reductase by Aldose Reductase Inhibitors. The inhibition of wild-type aldehyde reductase by alrestatin is competitive (K_{is} = 112 ± 12 μM) with the alcohol substrate in the reverse reaction and purely noncompetitive ($K_{is} = K_{ii} = K_i$ = 148 ± 12 μM) with the aldehyde substrate in the forward reaction. Such an inhibition pattern may be explained if the inhibitor preferentially binds to the E:$NADP^+$ complex rather than to the E:NADPH complex. The binding of AL1576, a better inhibitor of aldehyde reductase, which also exhibits noncompetitive inhibition in the forward reaction ($K_{is} = K_{ii} = K_i$ = 60 ± 6 nM), was measured by the ultrafiltration assay. The results (Table 5) show that AL1576 barely binds to the apoenzyme in the absence of coenzyme, but strongly binds to the E:$NADP^+$ complex and very weakly binds to the E:NADPH complex. Similar ultrafiltration experiments with the Y49H and H112Q mutants show that they bind AL1576 in the $NADP^+$ form, with virtually no binding to the apoenzyme or E:NADPH complex.

Table 6 compares the IC_{50} values of various aldose reductase inhibitors for the inhibition of aldehyde reductase, its H112Q mutant, and wild-type aldose reductase. AL1576 is the most potent aldehyde reductase inhibitor and has the highest specificity for aldehyde reductase as compared to aldose reductase. Tolrestat is the second most potent aldehyde reductase inhibitor, while alrestatin is the least potent inhibitor among all of the ARIs tested. The H112Q mutation considerably diminished enzyme affinity for the

inhibitors, as judged by the IC_{50} values (Table 6). The IC_{50} values for most inhibitors increased 50-fold on average, which corresponds to the elevated K_m for substrates exhibited by this mutant. AL1576 still remained the most potent inhibitor of the H112Q mutant. The IC_{50} for alrestatin was so high that it was not possible to measure it with a reasonable degree of accuracy.

DISCUSSION

Aldehyde reductase is a member of the NADPH-dependent aldo−keto reductase family, which includes aldose reductase (Bohren et al., 1989). These enzymes share a high degree of homology in their primary and secondary structures, substrate specificities, and kinetic mechanisms. Their catalytic mechanisms involve the introduction of the substrate to the E:NADPH complex, with subsequent hydride transfer from the nicotinamide ring to the carbonyl group of the substrate and the obligate addition of a proton to the substrate some time during the reaction to form the hydroxyl group of the alcohol product. Release of the alcohol product is followed by an enzyme conformational change, involving in part a nucleotide-clamping loop with release of the oxidized $NADP^+$ coenzyme and replacement with NADPH. The nucleotide exchange and its attendant enzyme conformational changes has been shown to be the rate-limiting step for the overall reaction of aldose reductase (Grimshaw et al., 1989; Kubiseski et al., 1992).

The crystal structure of aldose reductase shows that it is a β/α barrel enzyme (Rondeau et al., 1992) with the NADPH cofactor enfolded across the C-terminal end of the barrel by a loop of residues (Wilson et al., 1992). The 4-*pro*-*R*-hydrogen of the nicotinamide is exposed to solvent at the bottom of an active site pocket lined with hydrophobic residues, some of which are contributed by the loop enfolding the NADPH (Wilson et al., 1992; Harrison et al., 1994). Two residues, His110 and Tyr48, along with the C4 of the nicotinamide form a triangle at the bottom of the active site pocket. Our crystallographic studies identified the carboxylate moiety of citrate (a weak inhibitor of aldose reductase and a fortuitous component of the crystallization buffer) to be bound at the center of the plane of this equilateral triangle and showed that the crystal-bound cofactor is $NADP^+$ (Harrison et al., 1994). This anion-binding site was also found to bind other anions such as cacodylate, phosphate, and various inhibitors of aldose reductase (Ehrig et al., 1994). The inhibitor-binding site is thus a positively charged anion well formed by Tyr48, His110, and the nicotinamide ring (Harrison et al., 1994) that is involved in the binding of inhibitors and the chemistry of catalysis.

Central Roles of Tyr49 and Lys79 in the Active Site. In an earlier study, we determined that Tyr48 is the proton donor in the aldehyde reduction reaction catalyzed by aldose reductase (Bohren et al., 1994). Our studies showed that a Y48F mutant is totally inactive, while studies of a catalytically active Y48H mutant enzyme showed that a water molecule can replace the phenolic hydroxyl of Tyr48 as the source of the required proton. The crystal structure of the Y48H mutant revealed the location of a water molecule in precisely the space previously occupied by the hydroxyl of Tyr48 in the wild-type enzyme. Tyr48 is conserved throughout the aldo−keto reductase superfamily and corresponds to Tyr49 in aldehyde reductase. In the present study, mutation of this residue to phenylalanine, which conserves the hydrophobic properties and spatial fit of a tyrosine residue, yet eliminates the possibility of general acid catalysis by removing the tyrosyl hydroxyl group, also leads to a completely inactive enzyme. A histidine substitution for tyrosine 49 in aldehyde reductase (Y49H) also yields an inactive enzyme. Thus, unlike human aldose reductase, the geometry of the aldehyde reductase active site does not permit substitution for the Tyr49 hydroxyl function by some other element, such as the water molecule detected in the crystal structure of the Y48H aldose reductase mutant. Alternatively, if such a substitution does take place, it diminishes the catalytic efficiency for all the substrates to a greater extent than in aldose reductase, making it virtually impossible to detect any enzymatic activity.

The normal pK_a of a water-exposed tyrosine side chain is around 10.5, and we previously suggested that the proton donor function of Tyr48 in human aldose reductase is consistent with a downward shift in its pK_a to 8.4 imparted by a hydrogen-bonding/salt-bridge network formed by $Asp43^-/Lys77^+$ and Tyr48. A K77M mutation in human aldose reductase inactivates the enzyme (Tarle et al., 1993; Bohren et al., 1994). In this study, mutation of Lys79 (which corresponds to Lys77 in aldose reductase) to methionine (K79M) also yields an inactive enzyme, indicating that this residue plays a similarly critical role in aldehyde reductase catalysis. The pH profiles of k_{cat}/K_m for the reduction of DL-glyceraldehyde and *p*-carboxybenzaldehyde by human aldehyde reductase (Figure 2) show the ionization of a group with an apparent pK_a of 9.4. This pK_a can be ascribed to Tyr49, which apparently experiences a 1 log unit acidic shift in its pK_a due to its interaction with Lys79, a shift that is smaller than that found in aldose reductase (observed pK_a = 8.4). Again, these findings suggest subtle differences in the geometry of the aldehyde reductase active site.

Nucleotide-binding studies additionally showed that both the Tyr49 and Lys79 residues influence the mode of cofactor binding (see Table 4). The binding of $NADP^+$ to the Y49F mutant was severely impaired, as shown by fluorescence and ultrafiltration assays, whereas the NADPH-binding mode was very similar to that of the wild-type enzyme, as judged by its dissociation constant (K_d) and the maximal quenching of enzyme fluorescence at saturating conditions. The K79M mutant, on the other hand, exhibited a higher affinity for $NADP^+$ than for NADPH, with a K_{dNADPH} 10 times higher and a K_{dNADP^+} 2 times lower than those of the wild-type enzyme. This mutant protein also lacked the absorption band at 300 nm of the E:$NADP^+$ complex (Figure 4), and quenching of its fluorescence by both oxidized and reduced cofactors was low in comparison with the wild-type and other mutants. Thus, Lys79 appears to be intimately involved in the charge transfer interaction that determines the spectral and fluorescence signatures of E:nucleotide complexes and influences the mode of binding. In contrast, tighter NADPH binding and looser $NADP^+$ binding were observed with the Y49H, H112Q, and I298C aldehyde reductase mutants.

Aldehyde reductase binds the nucleotides more loosely than aldose reductase. The binding constants of wild-type aldehyde reductase for NADPH and $NADP^+$ are 13−60-fold higher, respectively, than the corresponding constants for aldose reductase (K_{dNADPH} = 130 and 10 nM and K_{dNADP^+} = 360 and 6 nM, respectively). Interestingly, whereas a K77M aldose reductase mutant also showed a reversed

affinity for the two forms of coenzymes with the K_{dNADPH} increased 6-fold and the K_{dNADP^+} decreased 2-fold (Tarle et al., 1993), the binding affinities of the Y48F, Y48H, H110A, and C298A aldose reductase mutants (Ehrig et al., 1994) were affected to a much lesser extent than those of the corresponding aldehyde reductase mutants. The contrasting behavior of the mutants of these residues in the two enzymes (Y48 and Y49, H110 and H112, and C298 and I298 in aldose and aldehyde reductases, respectively) indicates a major difference in the mode of nucleotide binding by the two enzymes, which is reflected only in part by the dissociation constants. Furthermore, these findings strongly suggest that Lys79 plays a hitherto unappreciated and important role in determining the mode of coenzyme binding in both enzymes.

His112 Is Important for Substrate Orientation. Our studies of aldose reductase showed that His110 directs the stereochemical orientation of substrates in the active site pocket (Bohren et al., 1994). Mutation of the corresponding residue in aldehyde reductase, His112, to glutamine caused a 3−100-fold drop in k_{cat} for a range of substrates and comparable increases in K_m. As a result, the catalytic efficiency (k_{cat}/K_m) decreased by 32−5000-fold (Table 2), indicating a similarly important role for the H112 residue in aldehyde reductase. Again, different substrates were affected to a different extent, suggesting a crucial role for this residue in determining the substrate specificity of aldehyde reductase. Aromatic substrates like *p*-nitrobenzaldehyde and *p*-carboxybenzaldehyde were greatly affected, while the polar substrates were less affected. This finding is consistent with the importance of His112 for the accommodation of aromatic substrates in an aldehyde reductase active site. However, it should be noted that His112 was substituted by a polar glutamine residue, which should preferentially interact with hydrophilic substrates, and that may be part of the reason why hydrophobic substrates were more strongly affected by the mutation. Similar changes were also seen in the H110Q aldose reductase mutant.

We also observed earlier that His110 plays an important role in the stereochemical orientation of 2-hydroxyaldehyde substrates within the active site pocket of aldose reductase (Bohren et al., 1994), as reflected by the wild-type enzyme's ability to distinguish between D-xylose and its stereoisomers L-xylose and D-lyxose. Indeed, the pH profiles of the wild-type aldehyde reductase (Figure 2) show that the catalytic efficiency, k_{cat}/K_m, for DL-glyceraldehyde decreases below pH 6, while the k_{cat}/K_m value for *p*-carboxybenzaldehyde does not change in this pH range. This drop in catalytic efficiency below pH 6 is attributable to the protonation of His112 that affects the DL-glyceraldehyde interaction and increases its K_m. In contrast, *p*-carboxybenzaldehyde does not possess a group at the C2-carbon atom that is capable of hydrogen bonding with the neutral histidine, and its k_{cat}/K_m thus is not affected below pH 6. Although the acidic drop in the DL-glyceraldehyde curve is shown by a single experimental point at pH 5.5, which was reproduced repeatedly and consistently, our suggestion that the His112 protonation state affects catalytic efficiency for 2-hydroxy aldehyde substrates seems plausible in view of the proposed role for this residue in orienting the substrates and by analogy with aldose reductase. The pH profile of the H112Q mutant determined with DL-glyceraldehyde does not exhibit a drop in the acidic region, reflecting the fact that glutamine is not ionizable. It should be noted that the glutamine amido group is still capable of forming a hydrogen bond with the C2-hydroxyl group of DL-glyceraldehyde or D-glucuronate (Table 2), and this interaction may account for the observation that these substrates are affected to a lesser extent by the H112Q mutation. We conclude that, as for the corresponding histidine in aldose reductase, His112 in aldehyde reductase also plays an important role in directing the specificities and stereochemical orientations of certain substrates within the active site pocket.

Roles of Ile298 and Val299 in the Active Site Pocket. The Cys298 residue plays a very important role in determining the thiol sensitivity and kinetic parameters of aldose reductase (Bohren & Gabbay, 1993) and appears to do so by a variety of interactions within the active site pocket (Gabbay et al., in preparation). The corresponding residue in aldehyde reductase may be either Ile298 or Val299. Mutations of either of these residues did not cause drastic changes in enzyme kinetics. The Ile298 mutation to alanine (I298A) did not appreciably change the k_{cat}, but increased the K_m for various substrates from 6- to 20-fold and decreased the catalytic efficiencies from 4- to 30-fold. The I298C mutant had even more modest changes, with 5−10-fold increases in K_m's and 2−9-fold decreases in catalytic efficiencies. The kinetic parameters of the V299C mutant were not significantly altered from those of the wild-type enzyme. Compared to the H112Q mutant, these changes were substrate-unspecific. Similar to the wild-type enzyme, neither the I298C nor the V299C mutant displayed any kinetically detectable sensitivity to β-mercaptoethanol. The lack of a major effect of mutations of the Ile298 and Val299 residues and the lack of thiol sensitivity in the cysteine mutations suggest that the organization or geometry of the active site pocket in aldehyde reductase differs from that of aldose reductase. We propose that these differences may be due to the longer C-terminal loop (Bohren et al., 1989), which we hypothesize forms a part of the active site pocket in aldehyde reductase. The C-terminal loop is unique for each of the aldo−keto reductases (Bruce et al., 1994), and we previously showed that it is critical for determining substrate specificity in aldose reductase (Bohren et al., 1992).

Catalytic Mechanism. Primary deuterium and solvent isotope effects (Table 3) indicate that the chemistry of the reaction is partially rate-limiting in the overall catalytic cycle of wild-type aldehyde reductase. The primary deuterium isotope effect measured with NADPD is significantly different from 1 for both k_{cat} and k_{cat}/K_m, indicating that hydride transfer is partially rate-limiting. The effect on k_{cat} is smaller than that on $k_{cat}/K_{m(aldehyde)}$, a term that comprises all of the steps in the catalytic cycle from the binding of aldehyde to the E:NADPH complex through the release of the alcohol product. The fact that the isotope effect on k_{cat}/K_m is larger than that on k_{cat} suggests that steps outside this part of the reaction sequence, i.e., nucleotide exchange and the associated enzyme isomerization, are partially rate-limiting for overall turnover. There was no solvent isotope effect on k_{cat}, although a significant effect was observed on k_{cat}/K_m (2.02 ± 0.06). If we use a value of 6.5 for ^Dk, the intrinsic isotope effect on hydride transfer based on that determined for aldose reductase (Grimshaw et al., unpublished), and a value of 8 for ^{D_2O}k determined for the solvent isotope effect on k_{cat}/K_m of the Y14F mutant of Δ^5-3-ketosteroid isomerase (Xue et al., 1991), then a simple calculation of the fractional rates (Northrop, 1975) would suggest about 23% rate

limitation of k_{cat}/K_m by hydride transfer and about 15% rate limitation by proton transfer, with the remainder contributed by other steps comprising k_{cat}/K_m. A similar calculation using the isotope effect on k_{cat} indicates that hydride transfer accounts for ~9% of limitation of the overall reaction velocity.

The conformational change associated with the release of $NADP^+$ was found to constitute the rate-limiting step in aldose reductase (Grimshaw et al., 1989; Kubiseski et al., 1992; Grimshaw et al., submitted for publication). The structural basis for this conformational change is the movement of a loop that enfolds the nucleotide and holds it tightly in place (Wilson et al., 1992). The apparent "acceleration" in the loop movement in aldehyde reductase (in comparison to aldose reductase) is most probably responsible for the generally 1 order of magnitude higher turnover numbers characteristic of this enzyme. As a consequence of this acceleration, the chemical steps appear to be more rate-limiting in the overall turnover rate of aldehyde reductase than of aldose reductase.

Separation of Hydride and Proton Transfer Steps in the H112Q Mutant. The H112Q mutant of aldehyde reductase catalyzes the reduction of DL-glyceraldehyde with k_{cat} values 6 times lower than that of the wild-type enzyme and with a significantly impaired catalytic efficiency (k_{cat}/K_m). The magnitude of the primary substrate deuterium isotope effect on k_{cat} in this mutant is only slightly higher than that of the wild type, suggesting approximately the same extent of overall rate limitation by hydride transfer. The isotope effect on k_{cat}/K_m was also similar to that of the wild-type enzyme. However, no solvent isotope effect on k_{cat}/K_m(glyceraldehyde) was observed, while there was a significant effect on k_{cat} (Table 3). This result indicates that the proton transfer described by the solvent isotope effect determines k_{cat}, but not k_{cat}/K_m; in other words, the proton transfer occurs after the first irreversible step of the reaction (Northrop, 1975). The shift in the Tyr49 pK_a in D_2O cannot explain this observation, since the experiments were performed at pH 7.0 where tyrosine is fully protonated and k_{cat}/K_m is on the plateau of the pH profile. The k_{cat}/K_m solvent effect could also be masked by a combination of the microscopic kinetic constants. However, the conditions leading to the masking of the solvent effect would also be expected to suppress the primary isotope effects on hydride transfer ($^Dk_{cat}/K_m$), and that is not the case. Different isotope effects on hydride transfer ($^Dk_{cat}/K_m$) and solvent isotope effect on proton transfer ($^{D_2O}k_{cat}/K_m$) indicate that H112Q enzyme catalysis must proceed via a stepwise mechanism, i.e., proton and hydride transfer occur in two distinct steps.

Strictly speaking, the proton transfer by itself comprises two steps in the catalytic sequence: the proton transfers from Tyr49 onto the substrate with subsequent reprotonation of the tyrosinate. Consequently, each of these steps may be the basis for the solvent isotope effect. Protonation of active site residues was suggested as a rate-limiting step for a fast substrate of pepsin (Rebholz & Northrop, 1991) and for proline racemase (Albery & Knowles, 1986). In the case of pepsin, the conclusion was supported by an observation similar to ours, i.e., the presence of a solvent isotope effect on k_{cat} but not on k_{cat}/K_m, and was attributed to the reprotonation of an active site aspartic residue—a prerequisite for the start of another catalytic cycle. Thus, slow protonation of Tyr49 in the aldehyde reductase H112Q mutant may give rise to the observed unusual solvent isotope effects. This explanation would be consistent with the observed pH profile of k_{cat} for this mutant, which is a straight line increasing at acidic pH (Figure 2). Indeed, if protonation were rate-limiting, k_{cat} should increase linearly with the logarithm of proton concentration. However, both pepsin and proline racemase are fast enzymes, with catalytic constants at least 10^4 times higher than that of H112Q mutant aldehyde reductase. Thus, the unusual solvent isotope effect for pepsin was observed only by using a substrate with k_{cat}/K_m in the range 10^7-10^8 M^{-1} s^{-1}, i.e., 7–8 orders of magnitude higher than what we observe with the H112Q mutant. Therefore, to be a rate-limiting step in the H112Q mutant, protonation has to become several orders of magnitude slower than in pepsin, which is unlikely.

The absence of a solvent effect on k_{cat}/K_m can be explained if we hypothesize that hydride transfer occurs first and irreversibly, followed by proton transfer. Since a reverse reaction cannot be experimentally detected with the H112Q enzyme, we can treat the chemical steps as virtually irreversible in a first approximation model. This situation is depicted by the following scheme where hydride transfer occurs first and is characterized by a step with the rate constant k_2, followed by the proton transfer characterized by k_3:

$$E + S \underset{k_{-1}}{\overset{k_1}{\rightleftharpoons}} ES \xrightarrow{k_2} X \xrightarrow{k_3} EP \underset{k_{-4}}{\overset{k_4}{\rightleftharpoons}} E + P$$

E represents the enzyme complex with NADPH, and the step EP ↔ E + P represents all steps from the dissociation of the alcohol product to the binding of reduced coenzyme. Steady-state treatment of this model shows that k_{cat}/K_m includes the steps from substrate binding until the formation of complex X, i.e., k_1, k_{-1}, and k_2, but not k_3. k_{cat}, however, includes k_3, as well as k_2 and k_4. Therefore, a primary isotope effect on hydride transfer (k_2) will be expressed in the steady-state equations for both k_{cat} and k_{cat}/K_m, whereas an isotope effect on proton transfer (k_3) will be expressed only in k_{cat}. This scheme ultimately leads to the following equations for the isotope effects:

$$^Dk_{cat}/K_m = \frac{k_{2H}/k_{2D} + k_{2H}/k_{-1}}{1 + k_{2H}/k_{-1}}$$

$$^Dk_{cat} = \frac{k_{2H}/k_{2D} + [(k_3 + k_4)/k_3k_4]k_{2H}}{1 + [(k_3 + k_4)/k_3k_4]k_{2H}}$$

$$^{D_2O}k_{cat}/K_m = 1$$

$$^{D_2O}k_{cat} = \frac{k_{3H}/k_{3D} + [(k_2 + k_4)/k_2k_4]k_{3H}}{1 + [(k_2 + k_4)/k_2k_4]k_{3H}}$$

These equations indicate that it is possible to observe primary isotope effects on hydride transfer and on both k_{cat} and k_{cat}/K_m, but with a solvent isotope effect observed only on k_{cat}. This is exactly the situation that we observe experimentally in the H112Q mutant ($^{D_2O}k_{cat}/K_m = 1$). The difference in this mutant from the wild-type aldehyde reductase is that, in the latter, hydride transfer and proton transfer occur in a reversible and probably concerted mode. In the H112Q mutant, due to the key histidine substitution,

the location of the substrate is less favorable for catalysis and proton transfer from Tyr49. Proton transfer to the carbonyl oxygen of the aldehyde substrate is impaired and slower than the hydride transfer at the moment when the chemical reaction is about to start. The intermediate product, X, in the model denotes the alcoholate anion, which is formed after hydride transfer from NADPH in a nucleophilic attack on the carbonyl of the aldehyde substrate. In other words, the process of hydride transfer develops the alcoholate anion, and the proton from Tyr49 transfers to the alcoholate anion instead of the carbonyl group, a process that is now favored due to the positive (proton) and negative (alcoholate) charges involved. This process can go fast despite the unfavorable location of Tyr49. Thus, in harmony with our conclusion that the His112 residue determines the substrate orientation in the active site, the H112Q substitution also brings about changes in the kinetic mechanism in the form of a two-step hydride and proton transfer instead of the probably concerted process in the wild-type enzyme.

Calculations similar to the ones made with the wild-type enzyme indicate that, in the H112Q mutant, hydride transfer accounts for 24% of the rate limitation of k_{cat}/K_m. According to the preceding scheme substrate binding contributes the other 76% of rate limitation. Thus, impaired substrate binding to the H112Q mutant is mainly responsible for the decrease in catalytic efficiency and the elevated K_m observed for this mutant. In the case of k_{cat}, hydride transfer and proton transfer account for 14% and 15% rate limitation, respectively. Thus, in the overall reaction, the chemistry of the H112Q mutant enzyme reaction contributes 29% (14% + 15%) rate limitation compared to only 9% in the wild-type enzyme, or a 3-fold increase. Considering that the k_{cat} for DL-glyceraldehyde decreased by 6-fold in the H112Q mutant, we can estimate that the chemical steps are approximately 20 times slower than for the wild-type enzyme, probably due to the hypothesized changes in the catalytic mechanism.

Inhibition by Aldose Reductase Inhibitors (ARIs). Several aldose reductase inhibitors have been developed and have undergone clinical human trials in the past 15 years for the prevention or reversal of several diabetic complications. These clinical trials, at best, have produced equivocal results so far, and some have resulted in significant side effects necessitating premature interruption. Although some of the problems may be attributed to the selection of end points and study designs, most of these inhibitors are nonspecific for aldose reductase and inhibit other enzymes in the aldo−keto reductase superfamily as well. In this study, we analyzed the mechanism and effectiveness of some of these inhibitors on aldehyde reductase. The IC_{50} values (Table 6) indicate that AL1576 is the most potent aldehyde reductase inhibitor, with a K_i in the nanomolar range, while alrestatin is the least potent, with K_i = 148 μM (Table 6). The order of inihibitory potency with aldehyde reductase is AL1576 > tolrestat > ponalrestat > sorbinil > FK366 > zopolrestat > alrestatin. These ARIs inhibit aldose reductase at a range of 60 nM to 2 μM, while the comparable range for aldehyde reductase is 60 nM to 148 μM. Of the two compounds currently undergoing clinical trials, it is clear that zopolrestat (Pfizer) has a much better specificity for aldose reductase than tolrestat (Wyeth-Ayerst), as reflected by the ratio of their IC_{50} values for the two enzymes (tolrestat and zopolrestat are 72- and 450-fold more potent, respectively, with aldose reductase than with aldehyde reductase; Table 6). The presence of a single aromatic ring system in tolrestat is the most likely basis for its potent inhibition of aldehyde reductase and its poor ability to discriminate between the two active site pockets (Ehrig et al., 1994). Zopolrestat has a flexible double aromatic ring system, which spans the active site pocket and anchors against residues contained in the C-terminal loop of aldose reductase (Wilson et al., 1993; Ehrig et al., 1994), a situation that may not be favored in aldehyde reductase due to differences in the C-terminal loop between the two enzymes in this region.

The basic mechanism of inhibition of aldehyde reductase by ARIs is similar to that of aldose reductase. Alrestatin exhibits a noncompetitive inhibition pattern using DL-glyceraldehyde as a substrate in the forward reaction and a competitive pattern using benzyl alcohol in the reverse reaction. AL1576 is also a noncompetitive inhibitor at small concentrations in the forward reaction, but becomes an uncompetitive inhibitor at a higher concentrations (80 nM, results not shown). However, the data for AL1576 were obtained under tight-binding conditions, i.e., the concentration of the inhibitor was comparable to that of the enzyme. This situation may have caused an essentially uncompetitive inhibition pattern to appear noncompetitive. For the same reason, the real inhibition constant for this inhibitor might be even lower than the apparent one reported here. Also, due to tight binding, the mode of AL1576 inhibition in the reverse reaction could not be determined. The inhibition pattern of aldehyde reductase, i.e., competitive in the reverse direction and non- to uncompetitive in the forward direction, is consistent with the inhibitors binding to the E:$NADP^+$ complex of aldehyde reductase. The same conclusion was reached by Wermuth (1990) in his study of aldehyde reductase inhibition by carboxylic acids and in our study of aldose reductase inhibition by alrestatin (Ehrig et al., 1994).

We further evaluated this point by directly measuring the binding of AL1576 to the different complexes of the enzyme by using an ultrafiltration assay. The results (Table 5) show that the inhibitor indeed binds preferentially to the wild-type E:$NADP^+$ complex, weakly to the E:NADPH complex, and not at all to the apoenzyme. There is no inhibitor binding to the Y49H mutant E:NADPH complex whatsoever, although there is appreciable binding to the E:$NADP^+$ complex, indicating the importance of the charged nature of the active site pocket. Inhibition studies of the H112Q enzymes show that the ARIs were still able to inhibit the H112Q mutant with similar relative potencies, although the inhibition potencies were impaired by 7−90-fold (Table 6). Since the H112Q mutation preferentially affected the catalytic efficiencies of aromatic substrates, and all of the tested inhibitors are also aromatic compounds, the diminished catalytic efficiency and inhibitory potencies indicate that the more affected inhibitors interact with His112 in an important way. This appears to be especially so with tolrestat, whose inihibition of the H112Q mutant is impaired by almost 90-fold. The inhibition by zopolrestat and FK366 is reduced by only 7- and 14-fold, respectively, suggesting that His112 is not as important to their binding, which suggests a different binding mode for these double aromatic ring system inhibitors (Ehrig et al., 1994).

Our results show that the mechanism of inhibition of aldehyde reductase by typical aldose reductase inhibitors

appears to be the same as that for aldose reductase (Ehrig et al., 1994), where we showed that negatively charged inhibitors bind to the positively charged anion-binding site (Harrison et al., 1994) in the active site pocket of aldose reductase. The high degree of crossover inhibition of aldose and aldehyde reductases by ARIs indicates the need to strive for both specificity and potency. Our data suggest that it should be possible to develop compounds with specificity, since zopolrestat has a 450-fold greater potency with aldose reductase than with aldehyde reductase.

These studies describe the kinetics, inhibition, and amino acid residues involved in the catalytic mechanism of aldehyde reductase. They indicate that the structure of the active site pocket in aldehyde reductase is significantly different from that of aldose reductase, which we postulate to result from participation of the C-terminal loop in the formation of the active site pocket. A major difference in the kinetic mechanism is the faster rate of cofactor exchange in aldehyde reductase, probably due to accelerated opening of the nucleotide-enfolding loop, making the chemical steps of the reaction appear to be partially rate-limiting. The chemical mechanism of aldehyde reductase catalysis appears to be quite similar to that of aldose reductase. A definitive description of the active site must await a high-resolution structure of the aldehyde reductase holoenzyme, which should facilitate the synthesis of highly specific inhibitors for each of these aldo−keto reductases.

ACKNOWLEDGMENT

We thank Ragini Shankar, Stephen Henry, and Charles Clasen for their technical assistance.

REFERENCES

Albery, W. J., & Knowles, J. R. (1986) *Biochemistry 25*, 2572−2577.
Bachur, N. R. (1976) *Science 193*, 595−597.
Bhatnagar, A., Das, B., Gavva, S. R., Cook, P. F., & Srivastava, S. K. (1988) *Arch. Biochem. Biophys. 261*, 264−274.
Birdsall, B., King, R. W., Wheeler, M. R., Lewis, C. A., Goode, S. R., Dunlap, R. B., & Roberts, G. C. K. (1983) *Anal. Biochem. 132*, 353−361.
Boghosian, R. A., & McGuinness, E. T. (1981) *Int. J. Biochem. 13*, 909−914.
Bohren, K. M., & Gabbay, K. H. (1993) in *Enzymology and Molecular Biology of Carbonyl Metabolism* (Weiner, H., Crabb, D. W., & Flynn, T. G., Eds.) Vol. 4, pp 267−277, Plenum, New York.
Bohren, K. M., Bullock, B., Wermuth, B., & Gabbay, K. H. (1989) *J. Biol. Chem. 264*, 9547−9551.
Bohren, K. M., Page, J. L., Shankar, R., Henry, S. P., & Gabbay, K. H. (1991) *J. Biol. Chem. 266*, 24031−24037.
Bohren, K. M., Grimshaw, C. E., & Gabbay, K. H. (1992) *J. Biol. Chem. 267*, 20965−20970.
Bohren, K. M., Grimshaw, C. E., Lai, C.-J., Harrison, D. H., Ringe, D., Petsko, G. A., & Gabbay, K. H. (1994) *Biochemistry 33*, 2021−2032.
Bruce, N. C., Willey, D. L., Coulson, A. F. W., & Jeffery, J. (1994) *Biochem. J. 299*, 805−811
Cleland, W. W. (1963) *Arch. Biochem. Biophys. 67*, 104−137.
Cleland, W. W. (1977) *Adv. Enzymol. 45*, 273−387.
Cleland, W. W. (1979) *Methods Enzymol. 63*, 103−138.
Davidson, W. S., & Flynn T. G. (1979) *Biochem. J. 177*, 595−601.
Davidson, W. S., Walton, D. J., & Flynn, T. G. (1977) *Comp. Biochem. Physiol. 60B*, 309−315.
De Jongh, K. S., Schofield, P. J., & Edwards, M. R. (1987) *Biochem. J. 242*, 143−150.
Dvornik, D. (1987) *Aldose reductase inhibition. An approach to the prevention of diabetic complications* (Port, D., Ed.) Biomedical Information Corporation, McGraw-Hill, New York.
Ehrig, T., Bohren, K. M., Prendergast, F. G., & Gabbay, K. H. (1994) *Biochemistry 33*, 7157−7165.
El-Kabbani, O., Green, N. C., Lin, G., Carson, M., Narayana, S. V. L., Moore, K. M., Flynn, T. G., & DeLucas, L. J. (1994) *Acta Crystallogr. D50*, 859−868.
Gabbay, K. H. (1973). *New Engl. J. Med. 288*, 831−836.
Garcia-Perez, A., & Burg, M. B. (1991) *Physiol. Rev. 71*, 1081−1115.
Gill, S. C., & von Hippel, P. H. (1989) *Anal. Biochem. 182*, 319−326.
Grimshaw, C. E., Shahbaz, M., Jahangiri, G., Putney, C. G., McKercher, S. R., & Mathur, E. J. (1989) *Biochemistry 28*, 5343−5353.
Harrison, D. H., Bohren, K. M., Ringe, D., Petsko, G. A., & Gabbay, K. H. (1994) *Biochemistry 33*, 2011−2020.
Hermes, J. D., Roeske, C. A., O'Leary, M. H., & Cleland, W. W. (1982) *Biochemistry 21*, 5106−5114.
Kador, P. F. (1988) *Med. Res. Rev. 8*, 325−352.
Kubiseski, T. J., Hyndman, D. J., Morjana, N. A., & Flynn, T. G. (1992) *J. Biol. Chem. 267*, 6510−6517.
Northrop, D. B. (1975) *Biochemistry 14*, 2644−2650.
Northrop, D. B. (1977) in *Isotope Effects on Enzyme-Catalyzed Reactions* (Cleland, W. W., O'Leary, M. H., & Northrop, D. B., Eds.) pp 122−152, University Park Press, Baltimore, MD.
Orr, G. A., & Blanchard, J. S. (1984) *Anal. Biochem. 142*, 232−234.
Pantaloni, D., & Dessen, P. (1969) *Eur. J. Biochem. 11*, 510−519.
Rebholz, K. L., & Northrop, D. B. (1991) *Biochem. Biophys. Res. Commun. 176*, 65−69.
Rizzo, V., Pande, A., & Luisi, P. L. (1987) in *Pyridine Nucleotides Coenzymes* (Dolphin, D., Poulson R., & Avramovic, O., Eds.) pp 100−154, Wiley, New York.
Rondeau, J.-M., Tete-Fâvier, F., Podjarny, A., Reyman, J.-M., Barth, P., Biellmann, J.-F., & Moras, D. (1992) *Nature 355*, 469−472.
Ryle, C. M., & Tipton, K. F. (1985) *Bichem. J. 227*, 621−627.
Salomaa, P., Schaleger, L. L., & Long, F. A. (1964) *J. Am. Chem. Soc. 86*, 1.
Stinson, R. A., & Holbrook, J. J. (1973) *Biochem. J. 131*, 719−728.
Tanimoto, T., Fukuda, H., Yamaha, T., & Tanaka, C. (1986) *Chem. Pharm. Bull. 34*, 4183−4189.
Tarle, I., Borhani, D. W., Wilson, D. K., Quiocho, F. A., & Petrash, J. M. (1993) *J. Biol. Chem. 268*, 25687−25693.
Viola, R. E., Cook, P. F., & Cleland, W. W. (1979) *Anal. Biochem. 96*, 334−340.
Von Wartburg, J.-P., & Wermuth, B. (1982) *Methods Enzymol. 89*, 506−513.
Wermuth, B. (1982) in *Enzymology of Carbonyl Metabolism: Aldehyde Dehydrogenase and Aldo/Keto Reductase*, pp 261−274, Alan R. Liss, Inc., New York.
Wermuth, B. (1990) in *Enzymology and Molecular Biology of Carbonyl Metabolism 3* (Weiner, H., et al., Eds.) pp 197−204, Plenum Press, New York.
Wermuth, B., Bürgisser, H., Bohren, K., & Von Wartburg, J.-P. (1982) *Eur. J. Biochem. 127*, 279−284.
Wilson, D. K., Bohren, K. M., Gabbay, K. H., & Quiocho, F. A. (1992) *Science 257*, 81−84.
Xue, L., Talalay, P., & Mildvan, A. S. (1991) *Biochemistry 30*, 10858−10865.

BI950957S